

Multi-object spectroscopy of low redshift EIS clusters. II. *

L.F. Olsen¹, L. Hansen¹, H.E. Jørgensen¹, C. Benoist³, L. da Costa², and M. Scodeggio⁴

¹ Copenhagen University Observatory, Juliane Maries Vej 30, DK-2100 Copenhagen, Denmark

² European Southern Observatory, Karl-Schwarzschild-Str. 2, D-85748 Garching b. München, Germany

³ Observatoire de la Côte d’Azur, CERGA, BP 229, 06304 Nice, cedex 4, France

⁴ Istituto di Fisica Cosmica - CNR, Milano, Italy

Received; accepted

Abstract. We present the results of carrying out multi-object spectroscopy in 10 EIS cluster fields. Based on the list of 345 galaxy redshifts we identify significant 3D-density enhancements. For 9 of the EIS clusters we identify significant 3D-concentrations corresponding to the originally detected cluster candidate. We find redshifts in the range $0.097 \leq z \leq 0.257$ which is in good agreement with the matched filter estimate of $z_{\text{MF}} = 0.2$. We estimate velocity dispersions in the range 219-1160 km/s for the confirmed clusters.

Key words. cosmology: observations – galaxies: distances and redshifts – galaxies: clusters: general

1. Introduction

The evolution of galaxy clusters’ properties, as well as that of their constituent galaxies, are important issues for contemporary cosmology and astrophysics. The demand for large samples of clusters of galaxies covering a large range in redshift has prompted systematic efforts to assemble catalogues of distant galaxy clusters (e.g. Gunn et al. 1986; Postman et al. 1996; Scodeggio et al. 1999; Gladders & Yee 2001; Gonzalez et al. 2001). The main goal behind such works is to assemble large samples of clusters with $z \gtrsim 0.5$ because at these redshift the evolutionary effects become more significant. However, another important issue in evolutionary studies is to have a well-defined comparison sample at lower redshifts. This sample can be taken from other surveys, but it would be preferable to build it from the same survey, in order to minimize the differences in selection effects.

This work is part of a major on-going confirmation effort to study all EIS cluster candidates (Olsen et al. 1999a,b; Scodeggio et al. 1999). This sample consists of 302 cluster candidates with estimated redshifts $0.2 \leq z_{\text{MF}} \leq 1.3$ and a median estimated redshift of $z_{\text{MF}} = 0.5$. The cluster candidates were identified using the matched filter technique originally suggested by Postman et al. (1996). The spectroscopic confirmation of the clusters was initiated by Ramella et al. (2000), who used the multi-object spectroscopy mode at the ESO 3.6m telescope at La Silla, Chile, to obtain confirmations of intermediate red-

shift candidates ($0.5 \lesssim z_{\text{MF}} \lesssim 0.7$). Benoist et al. (2002) presented the first results for the high redshift sample ($z \gtrsim 0.8$) with confirmation of three EIS clusters.

In this work we concentrate on the effort to build up the low redshift ($z_{\text{MF}} \leq 0.4$) reference sample for our future evolutionary studies that will combine the results for all redshifts. Of the entire EIS sample, 147 cluster candidates are at $z_{\text{MF}} \leq 0.4$. The first part of this low- z sample are the candidates at $z_{\text{MF}} = 0.2$ in patches A, B and D (Nonino et al. 1999) which consists of 34 candidates. The spectroscopic confirmation of the $z_{\text{MF}} = 0.2$ candidates was initiated by Hansen et al. (2002) who presented the first investigations of five patch D clusters of which 3 have $z_{\text{MF}} = 0.2$ and 2 have $z_{\text{MF}} = 0.3$. In this work we present the results for 10 additional cluster candidates increasing the $z_{\text{MF}} = 0.2$ sample to a total of 13 candidates corresponding to 37% of the entire sample with $z = 0.2$. With this work we complete the set of clusters in the first two patches (A and B).

2. Observations and data reduction

The observations were carried out at the Danish 1.54m telescope at La Silla, Chile. We used the Danish Faint Object Spectrograph and Camera (DFOSC) in the Multi-Object Spectroscopy (MOS)-mode. The field of view of DFOSC is $13'7 \times 13'7$ corresponding to 2.31Mpc at $z = 0.2$ (assuming $H_0 = 75\text{km/s/Mpc}$ and $q_0 = 0.5$, as was used for the original EIS cluster search, Olsen et al. 1999a) matching well the typical extent of galaxy clusters. Recent tests have shown that this instrument is suitable for carrying out MOS observations of cluster galaxies at $z \lesssim 0.4$

Send offprint requests to: L.F. Olsen, lisbeth@astro.ku.dk

* Based on observations made with the Danish 1.5-m telescope at ESO, La Silla, Chile

(Hansen et al. 2002). The effective field that could be covered with MOS slit masks was typically $11'0 \times 5'5$, depending on the exact configuration of galaxy positions in each field. The slit width was set to $2''$, and the slit length varied according to the extent of each galaxy. We used grism #4, giving a dispersion of $220\text{\AA}/\text{mm}$, and covering, on average, a wavelength range from 3800 to 7500 \AA . However, the useful range for each spectrum depends on the exact position of the slit with respect to the chip and the intrinsic galaxy spectrum. The resolution as determined from HeNe line spectra was found to be 16.6\AA FWHM.

For each cluster we created 2 or 3 slitmasks, targetting nearly all galaxies with $m_I \leq 19.5$, which roughly corresponds to $M^* + 2$ at $z = 0.2$. This procedure was chosen to avoid possible biases introduced by an additional color selection of the target galaxies. Furthermore, it assures that all clusters are treated similarly, even though not all of them are detected as concentrations in color and projected distribution (Olsen et al. 2001).

In Table 1 we list all the cluster candidates in patches A and B with $z_{\text{MF}} = 0.2$. In Col. 1 we give the cluster candidate identification name, in Cols. 2 and 3 the right ascension and declination (J2000), in Col. 4 the Λ_{cl} -richness (see Olsen et al. 1999a), in Col. 5 the Abell-like richness, N_R , and in Col. 6 the number of slitmasks for this object. The observations were carried out during three observing runs (August 2001, October 2001, and August 2002). Due to less than ideal observing conditions the candidate EISJ0049-2931, which coincides with the cluster Abell S84, was not observed. This is not a major draw back for the program conclusions, since the aim is to obtain spectroscopic confirmations for the cluster candidates and for this one the redshift is already available in the literature ($z=0.11$, Abell et al. 1989).

The presence of newly installed calibration lamps in the sky baffle cover allowed us to carry out both the flat field and arc-calibration exposures on the same telescope positions as the science exposures. A calibration set consisted of one HeNe lamp exposure and three flat field exposures, while the entire observing sequence for each slitmask consisted of a calibration, $2 \times 15\text{min}$ science exposures, a calibration, $2 \times 15\text{min}$ science exposures and a calibration. This resulted in 60min on-sky exposures for each slitmask.

The data reduction was performed using the IRAF¹ package. The CCD bias level was determined from over-scan regions and subtracted. The flatfielding was carried out using the two sets of flatfields obtained immediately before and after each observation. This procedure has significantly improved the flatfielding of the exposures compared to what was possible in the setup phase of the MOS-mode at DFOSC. The newly installed flat field lamp together with the adopted observing procedure has allowed

a good flatfielding and reliable wavelength calibration for all the obtained spectra.

After the basic reductions we used standard procedures to extract the spectra and to obtain redshifts by Fourier cross-correlating our spectra with standard galaxy spectra templates from Kinney et al. (1996). Hansen et al. (2002) describes the reduction procedures in more detail. For the cross-correlation the template spectra were always redshifted close to the redshift under consideration. Whenever a peak in the correlation function was accepted as real or possibly real, the observed spectrum was inspected and compared to the expected positions of the most prominent spectral features. We demanded that some features like the Ca H and K lines, the 4000 \AA break, or emission lines should be identified before a determination was accepted as certain. If no convincing features were found, but the correlation peak appeared real, we mark the z -value with a colon (“:”) in Tables A.1-A.10.

The accuracy of the measured redshifts are influenced by the limited resolution, signal-to-noise, fringing and possible systematic errors in the wavelength transformation. These error sources vary from spectrum to spectrum. In Hansen et al. (2002) we estimate the error of the measured galaxy redshifts to be $\sigma_z \approx 0.0005$.

In a small number of cases the spectrum was affected by the presence of defects on the CCD chip, contamination by scattered light, or was simply too weak to yield a redshift determination. Still our completeness is very good, as shown in Fig. 1. The plots are based on all galaxies in the EIS galaxy catalogs (Nonino et al. 1999; Prandoni et al. 1999) with $I \lesssim 20.5$ (Vega system). The upper panel shows, as a function of magnitude, the target completeness, meaning the ratio of targeted to all galaxies within the region where slits were placed. It can be seen that at $I \lesssim 19$ we target 70% of all the galaxies, while at fainter magnitudes the completeness decreases steadily, going to zero at $I = 20.5$. In terms of obtaining redshifts for the targeted galaxies the lower panel shows the fraction of spectra for which redshifts could be determined. This shows that at $I \lesssim 18.5$ essentially all spectra yield redshifts while at fainter magnitudes the fraction of spectra for which redshifts are obtained drops to 75%. This efficiency in determining redshifts shows the adequacy of the chosen instrument for this type of project.

3. Results

Tables A.1 through A.10 give the measured redshifts for all the galaxies. The positions and photometry are from Nonino et al. (1999) and Prandoni et al. (1999). Magnitudes are total magnitudes determined by SExtractor (MAG_AUTO, Bertin & Arnouts 1996), and additionally corrected for interstellar extinction as described by Olsen (2000). In the tables an attached “:” represents a less secure redshift as described above, and an “e” indicates that the galaxy has one or more emission lines. The galaxies with redshifts in bold face are the ones considered members of the clusters.

¹ IRAF is distributed by the National Optical Astronomy Observatories, which is operated by AURA Inc. under contract with NSF.

Table 1. Cluster candidates selected for observations.

Field ^a	α_{J2000}	δ_{J2000}	Λ_{cl}	N_R	#masks
EISJ0045-2923	00:45:14.4	-29:23:43.4	33.8	100	3
EISJ0046-2925	00:46:07.4	-29:25:42.2	44.4	26	2
EISJ0049-2931	00:49:23.1	-29:31:56.8	84.2	48	not observed, see text
EISJ0052-2923	00:52:59.6	-29:23:14.1	26.7	14	2
EISJ2237-3932	22:37:45.3	-39:32:11.8	30.1	42	3
EISJ2241-3949	22:41:42.1	-39:49:14.6	47.9	30	3
EISJ2243-4013	22:43:01.3	-40:13:58.2	36.3	16	2
EISJ2243-4025	22:43:23.8	-40:25:49.9	28.9	6	3
EISJ2244-3955	22:44:23.2	-39:55:23.6	41.7	20	2
EISJ2245-3952	22:45:13.6	-39:52:21.9	32.6	12	2
EISJ2246-4012A	22:46:30.1	-40:12:48.4	34.6	19	3

^a Here we have added a “J” in the name to conform with international standards. This notation will be used throughout this work. The EIS identification is the same except for this “J”.

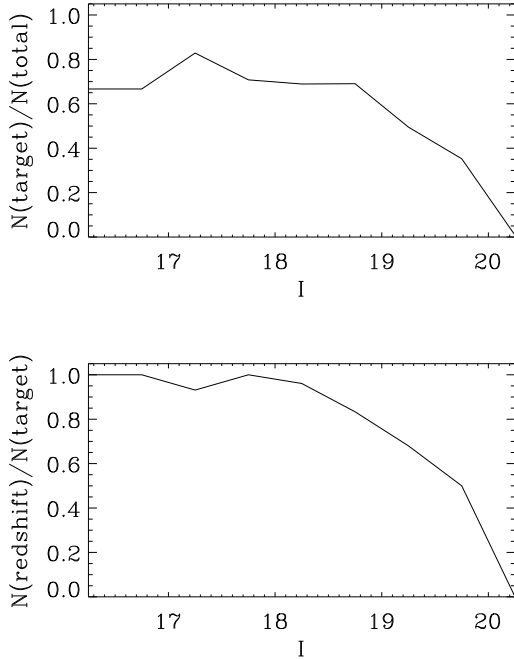


Fig. 1. Completeness in obtaining redshifts as function of magnitude. The upper panel shows the targeted fraction of all EIS galaxies within the regions covered by slits. The lower panel shows the fraction of targeted galaxies for which redshifts were determined.

We have secured between 19 and 61 redshifts per cluster field. In Fig. 2 we present the redshift distributions for each field as indicated. In the upper part of each panel we show the individual redshifts and in the lower part the redshift distribution in bins of $\Delta z = 0.01$. The solid histograms indicate groups that have been identified from the analysis of the redshift distribution as discussed below.

From the figure one can immediately see the presence of concentrations in all the cluster fields. In some fields

one obvious peak in the distribution is found indicating the presence of a cluster, while in others a series of less rich groups is found, possibly indicating that this detection is the result of a superposition of smaller systems. But it is interesting to note that in all the cluster fields we find concentrations in redshift space.

To identify systems in three-dimensional space we have used the “gap”-technique of Katgert et al. (1996). The “gap”-technique identifies gaps in the redshift distribution larger than a certain size to separate individual groups. In this analysis we have adopted a redshift gap of $\Delta z = 0.005 \cdot (1 + z)$ corresponding to 1500 km/s in the restframe. With this method we find a total of 30 groups with at least three members, scattered over all the cluster fields with between 1 and 5 groups per field. Table 2 lists the groups that we find significant as described below. The table gives for each group in Col. 1 the Cluster Field, Col. 2 the number of member galaxies, Cols. 3 and 4 the coordinates, Col. 5 the mean redshift, Col. 6 the restframe velocity dispersion in km/s corrected for the estimated error, Cols. 7 and 8 significances determined in two different ways as discussed below. We list all groups that have at least one of the significances larger than 99%.

For assessing the significance of these groups we have used two methods, one based on the redshift distribution from the CNOC2 0223+00 catalog (Yee et al. 2000), and another one based on the 3-dimensional galaxy distribution obtained from the 2dF Galaxy Redshift Survey (2dFGRS, Colless et al. 2001). In the first case we restrict ourselves to using only galaxies with measured redshift and I magnitude brighter than 19.5 corresponding to where we have about 50% completeness in the present survey. For each of the groups we identified in the redshift survey, we draw 1000 sets of galaxies from the CNOC2 survey. The sample size for the sets is taken to be the same as was measured in the field of the group. The redshift sample is now run through our group finding method. The identified field-groups are used to determine the distribution of

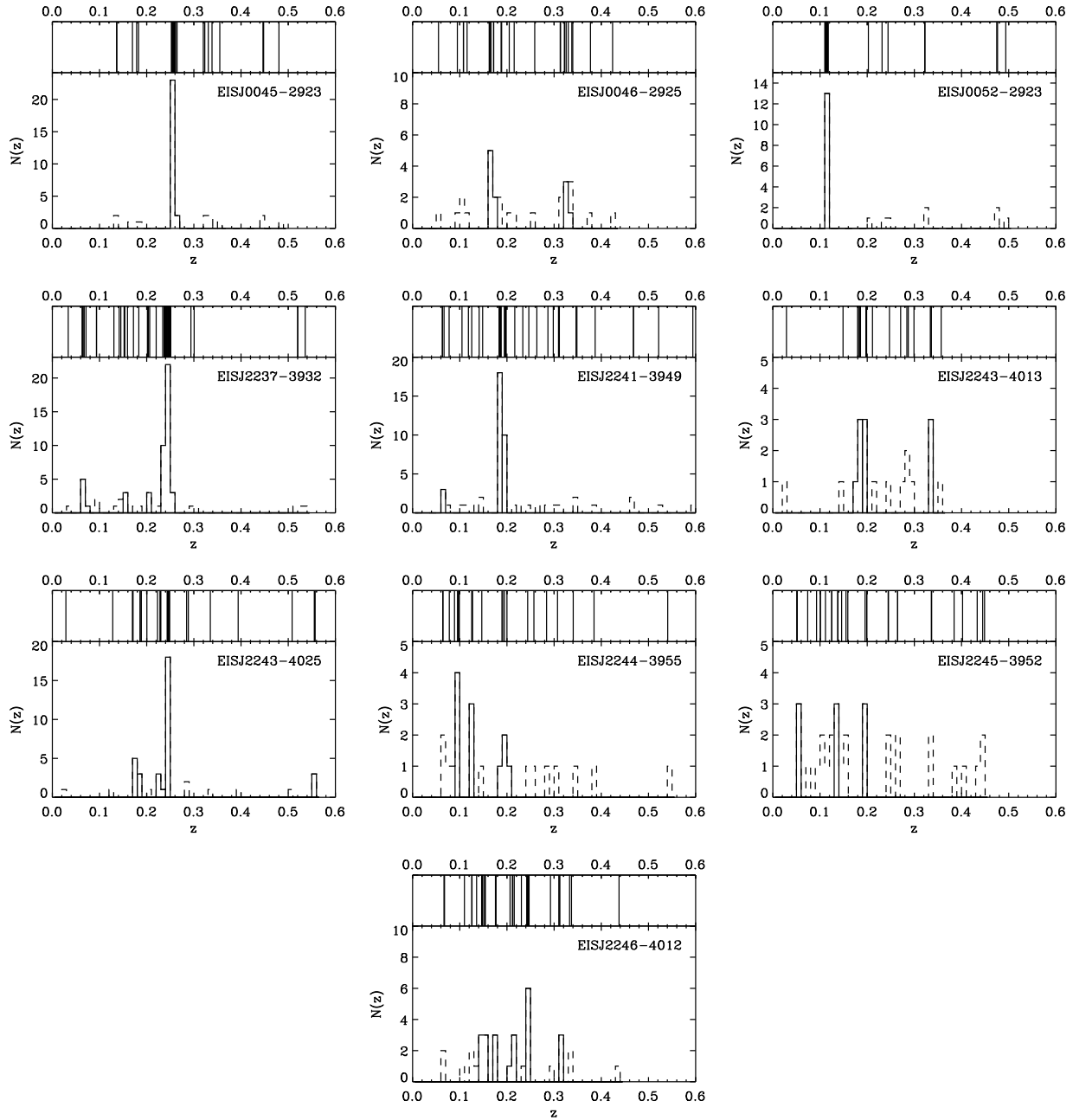


Fig. 2. Redshift distributions for the 10 observed cluster fields as indicated in each panel. Note that the scale of the y-axis differs between the panels. The upper panels show bar diagrams of the measured redshifts, while the lower panels give the corresponding histograms of the redshift distributions (dashed line). The solid lines mark the detected groups.

“number of member galaxies per group” for field galaxies. From this we derive the probability of finding a field-group with at least the same number of galaxies as we find in our redshift survey. However, the redshift distribution of field galaxies is not uniform, mainly because of our magnitude limit, and therefore the probability of finding a group with n -members is not constant in z . Therefore we restrict the derived probability to be within a redshift interval of $\Delta z = \pm 0.025$ from the redshift of the group. So the fi-

nally determined probability is the probability of having an equally rich or richer group within $\Delta z = \pm 0.025$. We compute the significance as the difference between unity and the derived probability. This significance is listed as σ_1 in Table 2.

The second approach is based on 2dFGRS. This survey is not as deep as ours but it provides us with a larger coverage and therefore is useful to investigate the real 3D distribution of the field galaxies. In this case we estimate

Table 2. Identified groups with a significance of at least 99% as obtained by at least one of the employed methods. The ones in bold face are the ones we interpret as causing the cluster detection as discussed in the text. The meaning of the missing σ_v 's is described in the text.

Cluster Field	Members	α (J2000)	δ (J2000)	z	σ_v [km/s]	σ_1 [%]	σ_2 [%]
EISJ0045-2923	25	00 45 15.6	-29 23 26.1	0.257	673	99.9	99.9
EISJ0046-2925	7	00 46 14.4	-29 27 17.0	0.167	981	99.9	99.3
EISJ0052-2923	13	00 52 52.1	-29 22 58.3	0.114	612	99.9	99.9
EISJ2237-3932	35	22 37 54.1	-39 33 32.1	0.244	1160	99.9	99.9
<i>EISJ2237-3932</i>	<i>6</i>	<i>22 37 35.2</i>	<i>-39 31 29.7</i>	<i>0.066</i>	<i>856</i>	<i>99.9</i>	<i>99.9</i>
EISJ2241-3949	18	22 41 48.2	-39 49 42.5	0.185	219	99.9	99.9
<i>EISJ2241-3949</i>	<i>10</i>	<i>22 41 43.9</i>	<i>-39 49 41.2</i>	<i>0.196</i>	<i>247</i>	<i>99.8</i>	<i>99.9</i>
<i>EISJ2241-3949</i>	<i>3</i>	<i>22 41 44.6</i>	<i>-39 48 41.9</i>	<i>0.064</i>	<i>552</i>	<i>99.8</i>	<i>99.7</i>
EISJ2243-4013	4	22 42 57.8	-40 15 45.7	0.183	680	98.1	99.7
EISJ2243-4025	18	22 43 33.4	-40 25 54.3	0.246	283	99.9	99.9
<i>EISJ2243-4025</i>	<i>5</i>	<i>22 43 37.9</i>	<i>-40 25 48.2</i>	<i>0.171</i>	-	<i>99.6</i>	<i>97.5</i>
<i>EISJ2243-4025</i>	<i>3</i>	<i>22 43 23.7</i>	<i>-40 25 12.5</i>	<i>0.556</i>	<i>137</i>	<i>99.8</i>	<i>61.9</i>
EISJ2244-3955	4	22 44 27.8	-39 56 1.8	0.097	429	99.9	99.6
<i>EISJ2245-3952</i>	<i>3</i>	<i>22 44 59.2</i>	<i>-39 53 14.6</i>	<i>0.051</i>	-	<i>99.8</i>	<i>99.9</i>
EISJ2246-4012A	6	22 46 40.9	-40 14 47.8	0.150	870	99.8	99.6

the probability that we find a (3D) region that contains at least the same number of galaxies as the group in question. For each of our identified groups we select 1000 random galaxies in the 2dFGRS catalog. Each galaxy provides us with a position and a redshift. Around this position we construct a cylinder for counting galaxies. To construct the cylinder we determine the physical size of the surveyed area at the redshift of the group. Now the cylinder is constructed to have a physical base-area corresponding to the area of the surveyed field but computed at the redshift of the 2dFGRS galaxy. The depth of the cylinder is determined to be the corresponding diameter of the base-area. Within each such cylinder we record the number of galaxies. From these 1000 randomly chosen volumes we determine the distribution of number of galaxies in order to obtain the probability of finding the same number of galaxies as in a particular group. The significance of the group is found as the difference between unity and the derived probability and is listed in Table 2 as σ_2 .

As said above, in Table 2 we include all the groups with a significance larger than 99% in one of the methods. In general, we find that the two methods agree quite well. However, in four cases we do find that one method would include the group and another one would exclude the group from the list. For three of these cases it is found that the other significance in the method that would have led to exclusion is only marginally lower. In one case we do find an extremely low significance based on the 2dFGRS data, but a high significance in the CNOC2 based method. For this group the redshift is $z = 0.556$ which is very high in the light of our limiting magnitude of $I = 19.5$ therefore the high significance is due to the redshift dependence. Taken over all redshifts a group of 3 galaxies is not very significant which is also seen in the 2dFGRS result.

For each cluster field we show in Fig. 3 the positions of those galaxies that are members of significant

density enhancements. The different symbols indicate different groups. In six cases (EISJ0045-2923, EISJ0046-2925, EISJ0052-2923, EISJ2237-3932, EISJ2241-3949, EISJ2243-4025) we find that the detected cluster is dominating the field and thus we interpret these as robust confirmations of the EIS clusters. In the case of EISJ2241-3949 the region, however, seems somewhat complicated by two groups at almost the same redshift. The smaller one at only slightly higher redshift is marked in open symbols in the figure. In three cases (EISJ2243-4013, EISJ2244-3955, EISJ2246-4012A) we find quite significant detections, even though the EISJ2243-4013 is only marginally significant in the CNOC2 method. These three detections are rather poor and slightly offset with respect to the EIS position, but we still believe that these clusters are the ones detected in the EIS catalog, thus we count them as confirmed clusters. However, it may very well be that the characteristics like richness and position, derived by the matched filter technique and reproduced in Table 1, is severely affected by other galaxies along the line of sight. In the case of EISJ2245-3952 the detected group has a high significance by both methods, however, the group is very offset compared to the EIS cluster candidate and furthermore the redshift is only $z = 0.051$, so we do not consider this cluster confirmed.

In total we therefore consider 9 clusters confirmed (marked in bold face in Table 2). For these nine we compute a mean redshift of $z_{spec} = 0.183 \pm 0.058$ in good agreement with the one estimated from the matched filter detections (all the cluster candidates had estimated redshifts of $z_{MF} = 0.2$).

The field-of-view used here covering roughly $10'$ corresponds to approximately 2Mpc ($H_0 = 75\text{km/s/Mpc}$, $q_0 = 0.5$) at $z = 0.2$. This field size corresponds well to the expected size of galaxy clusters. Since we only trace the brighter part of galaxy clusters we would expect to see

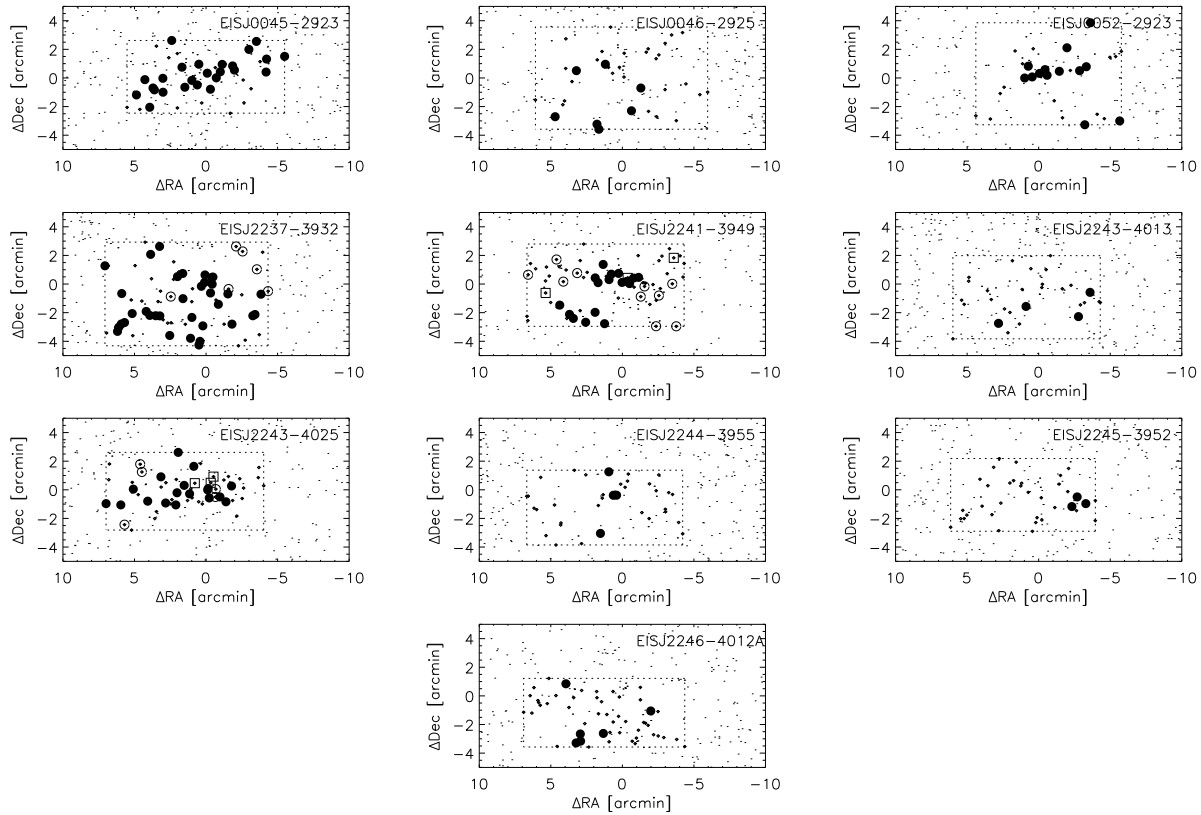


Fig. 3. Projected distributions of $I < 19.5$ galaxies (small dots) in each of the cluster fields as indicated in each panel. The matched filter center of the cluster is in the center of the plots. The dashed line mark the region covered by the MOS-masks, in some cases the MOS-masks are not centered on the cluster center due to the distribution of the bright galaxies. The small squares mark all the targeted galaxies. The filled circles mark the main group in each panel, while the large open symbols mark the other groups with one symbol per group.

mainly the central parts of the cluster, while in three cases (EISJ0045-2923, EISJ2237-3932, EISJ2243-4025) the clusters seem to extend over almost the entire surveyed field. This could either be caused (1) by the clusters being relatively closer to us (for instance at $z \sim 0.1$), (2) by unusually rich clusters with the bright galaxies widely spread in the sky, or possibly (3) by the detection of parts of filaments rather than galaxy clusters. The first hypothesis can be ruled out since in all three cases the redshift is $z \sim 0.25$, and thus not being closer than expected. The other two options are hard to verify from these data, even though all three cases are among the richer systems (the ones with the largest number of member galaxies) found in this work. It is however interesting that all of the systems are at almost the same redshift. A full understanding of this would require both deeper and more extended surveys.

In Table 2 we also list the computed velocity dispersions. The velocity dispersions are corrected for the estimated errors of $\delta z = 0.0005$ (see Hansen et al. 2002), and converted to restframe velocity dispersions by dividing by $(1+z)$. In a few cases we do not list the velocity dispersion which indicates that the measured raw velocity dispersion is smaller than 150km/s corresponding to the estimated

error. In all those cases the groups are rather small. For the groups with only very few members the velocity dispersion may not give a good estimate of the mass of the systems, however, the huge range of velocity dispersions indicates that the EIS cluster catalog covers a large range of properties of galaxy clusters. Therefore, the catalog will serve as a good basis for studying evolutionary effects for the entire population of clusters.

4. Conclusions

We have presented a set of 345 new redshift determinations for galaxies in ten EIS cluster fields. In 9 of these fields we find 3D-density enhancements that corresponds to the EIS clusters. Thus we find that in this relatively small sample of clusters we have a rate of $\sim 10\%$ false detections. This number will be further discussed when we have assembled the entire sample of spectra for the $z_{\text{MF}} = 0.2$ EIS cluster candidates in the three considered patches (A, B and D). If it holds we will collect a set of about 30 clusters at $z \sim 0.2$ to be used as a first step in evolutionary studies based on the EIS cluster catalog. We furthermore find that the redshift estimates by the matched filter method is in good agreement with the

ones obtained spectroscopically. The velocity dispersions indicate that the catalog covers a large range of cluster properties.

Acknowledgements. We thank John Pritchard, Lisa Germany and Ivo Saviane for making the pre-imaging observations of the fields. We would also like to thank the 2p2 team, La Silla, for their support at any time during the observations. We are also in debt to Morten Liborius Jensen for preparing the slit masks. This work has been supported by The Danish Board for Astronomical Research. LFO thanks the Carlsberg Foundation for financial support.

References

- Abell, G., Corwin, H., & Olowin, R. 1989, *ApJS*, 70, 1
 Benoist, C., da Costa, L., Jørgensen, H., et al. 2002, *A&A*, 394, 1
 Bertin, E. & Arnouts, S. 1996, *A&AS*, 117, 393
 Colless, M., Gavin, D., Maddox, S., et al. 2001, *MNRAS*, 328, 1039
 Gladders, M. & Yee, H. 2001, in *ASP Conf. Series*, Vol. 232, *The New Era of Wide Field Astronomy* (Astronomical Society of the Pacific), 126
 Gonzalez, A., Zaritsky, D., Dalcanton, J., & Nelson, A. 2001, *ApJS*, 137, 117
 Gunn, J., Hoessel, J., & Oke, J. 1986, *ApJ*, 306, 30
 Hansen, L., Olsen, L., & Jørgensen, H. 2002, *A&A*, 388
 Katgert, P., Mazure, A., Perea, J., et al. 1996, *A&A*, 310
 Kinney, A., Calzetta, D., Bohlin, R., et al. 1996, *ApJ*, 467, 38
 Nonino, M., Bertin, E., da Costa, L., et al. 1999, *A&AS*, 137, 51
 Olsen, L., Benoist, C., da Costa, L., et al. 2001, *A&A*, 380, 460
 Olsen, L. F. 2000, PhD thesis, Copenhagen University Observatory
 Olsen, L. F., Scodeggio, M., da Costa, L., et al. 1999a, *A&A*, 345, 681
 —. 1999b, *A&A*, 345, 363
 Postman, M., Lubin, L., Gunn, J., et al. 1996, *AJ*, 111, 615
 Prandoni, I., Wichmann, R., da Costa, L., et al. 1999, *A&A*, 345, 448
 Ramella, M., Biviano, A., Boschin, W., et al. 2000, *A&A*, 360, 861
 Scodeggio, M., Olsen, L. F., da Costa, L., et al. 1999, *A&AS*, 137, 83
 Yee, H., Morris, S., Lin, H., et al. 2000, *ApJS*, 129, 475

Appendix A: Measured redshifts

Table A.1. Redshifts obtained in the EISJ0045-2923 field. Here and in the following tables an attached “.” represents a less secure redshift as described in the text, and an “e” represents that the galaxy has one or more emission lines. The galaxies with redshifts in bold face are the ones considered members of the cluster.

	α (J2000)	δ (J2000)	l	z
1	00:44:58.244	-29:21:10.20	18.70	0.2595
2	00:44:49.194	-29:22:12.77	17.23	0.2563
3	00:45:00.653	-29:21:43.71	19.45	0.2564:
4	00:44:49.431	-29:22:24.31	18.08	0.1787
5	00:44:54.988	-29:22:24.26	17.81	0.2566
6	00:44:57.079	-29:22:34.95	18.27	0.1361e
7	00:45:05.872	-29:22:53.03	18.84	0.2566
8	00:45:05.298	-29:23:10.38	18.55	0.2614
9	00:44:55.146	-29:23:18.70	18.42	0.2575e
10	00:45:02.491	-29:23:51.99	19.95	0.3385e
11	00:45:15.789	-29:25:28.17	18.76	0.4479
12	00:45:06.614	-29:26:11.01	18.58	0.3200e
13	00:45:08.261	-29:22:45.04	16.55	0.1828e
14	00:45:23.627	-29:22:00.88	18.59	0.1368e
15	00:45:09.216	-29:22:46.49	17.89	0.2586
16	00:45:26.346	-29:22:18.45	18.27	0.1698
17	00:45:16.708	-29:22:45.86	18.28	0.2578
18	00:45:18.963	-29:23:53.73	16.38	0.2572
19	00:45:11.432	-29:23:00.03	18.87	0.4465:
20	00:45:22.118	-29:22:58.33	18.33	0.2546
21	00:45:14.003	-29:23:23.38	19.85	0.2551:
22	00:45:09.830	-29:23:17.61	19.33	0.2573
23	00:45:28.259	-29:23:44.88	18.07	0.2529
24	00:45:11.115	-29:23:42.82	19.46	0.2542
25	00:45:34.024	-29:23:50.47	19.58	0.2585
26	00:45:21.197	-29:24:22.31	17.74	0.2529
27	00:45:31.420	-29:24:25.58	18.18	0.2588
28	00:45:17.220	-29:24:12.70	18.27	0.2644
29	00:45:30.082	-29:24:32.86	19.30	0.4804
30	00:45:12.996	-29:24:30.78	19.40	0.2600
31	00:45:30.980	-29:24:33.30	19.36	0.2531:
32	00:45:36.724	-29:24:54.63	17.24	0.2585e
33	00:45:28.202	-29:24:43.30	18.45	0.2530
34	00:45:37.375	-29:24:43.14	19.52	0.3306
35	00:45:35.645	-29:25:54.91	18.56	0.3550
36	00:45:39.744	-29:25:46.61	18.17	0.3232e
37	00:45:32.465	-29:25:46.35	18.55	0.2585
38	00:45:25.414	-29:21:06.27	17.71	0.2537e

Table A.2. Redshifts obtained in the EISJ0046-2925 field.

	α (J2000)	δ (J2000)	I	z
1	00:46:14.951	-29:29:17.27	17.95	0.1654e
2	00:45:42.551	-29:26:52.16	18.28	0.2589
3	00:45:40.042	-29:26:41.50	19.42	0.4240
4	00:46:01.480	-29:26:24.45	17.74	0.1627
5	00:45:59.021	-29:28:02.16	17.61	0.2049
6	00:46:04.492	-29:27:59.84	18.93	0.1625
7	00:45:56.432	-29:28:24.52	18.04	0.3375
8	00:45:51.612	-29:22:41.96	15.64	0.0549e
9	00:45:48.104	-29:22:31.89	17.70	0.2153
10	00:46:25.554	-29:22:58.08	17.99	0.3395
11	00:45:53.694	-29:23:16.67	16.64	0.1076
12	00:46:06.843	-29:23:58.44	17.47	0.1888:
13	00:45:59.145	-29:23:40.03	18.77	0.3129
14	00:45:59.752	-29:23:54.02	17.97	0.1876:
15	00:45:55.714	-29:24:05.55	18.90	0.1080
16	00:46:15.485	-29:24:26.26	19.41	0.3137e
17	00:46:12.872	-29:24:44.92	19.04	0.1716e
18	00:46:08.371	-29:24:57.29	17.21	0.0949
19	00:46:06.907	-29:25:38.23	15.99	0.1155
20	00:46:25.602	-29:25:02.17	19.32	0.3256e
21	00:46:22.177	-29:25:11.67	19.31	0.1720
22	00:46:10.557	-29:25:22.46	19.55	0.3770:
23	00:46:23.588	-29:25:57.26	19.01	0.3300e
24	00:46:15.564	-29:28:56.14	17.69	0.1655e
25	00:46:35.311	-29:27:14.27	18.17	0.3225
26	00:46:26.523	-29:27:34.40	18.08	0.3217
27	00:46:28.986	-29:28:24.68	17.77	0.1662

Table A.3. Redshifts obtained in the EISJ0052-2923 field.

	α (J2000)	δ (J2000)	I	z
1	00:52:33.556	-29:26:14.35	16.39	0.1134
2	00:52:57.513	-29:22:39.14	14.87	0.1135
3	00:53:02.889	-29:22:24.90	17.91	0.1116
4	00:52:46.426	-29:22:43.69	17.62	0.1102
5	00:52:44.280	-29:22:27.04	19.70	0.1155:
6	00:52:52.925	-29:22:46.19	17.23	0.1167
7	00:52:49.409	-29:22:42.36	19.95	0.4937:
8	00:52:56.850	-29:23:02.88	17.67	0.1163
9	00:53:01.636	-29:23:09.79	18.49	0.1138e
10	00:52:54.573	-29:24:49.68	18.84	0.4746
11	00:52:51.916	-29:26:01.13	18.74	0.2025
12	00:52:44.753	-29:26:30.38	17.43	0.1156
13	00:53:19.717	-29:25:52.91	18.50	0.2315e
14	00:53:15.060	-29:26:06.17	18.59	0.4763
15	00:53:07.130	-29:21:20.80	19.74	0.2442
16	00:53:04.746	-29:22:14.64	18.75	0.3226
17	00:53:04.042	-29:23:14.37	16.89	0.1128
18	00:53:11.892	-29:24:19.21	19.02	0.3219
19	00:52:42.921	-29:19:22.67	17.84	0.1161
20	00:52:50.482	-29:21:07.64	17.05	0.1108
21	00:52:59.294	-29:22:55.16	16.09	0.1173

Table A.4. Redshifts obtained in the EISJ2237-3932 field.

	α (J2000)	δ (J2000)	I	z
1	22:37:26.882	-39:31:10.05	18.55	0.0675e
2	22:37:22.822	-39:32:41.62	18.23	0.0636e
3	22:37:37.142	-39:32:32.77	19.36	0.0667:
4	22:37:25.395	-39:32:54.56	18.91	0.2493
5	22:37:37.389	-39:32:53.30	19.40	0.2455
6	22:37:32.345	-39:32:56.93	19.90	0.2938:
7	22:37:41.710	-39:33:18.67	18.75	0.2037e
8	22:37:40.849	-39:33:36.93	19.18	0.2426e
9	22:37:27.567	-39:34:19.54	18.97	0.2421e
10	22:37:28.349	-39:34:24.81	17.58	0.2433e
11	22:37:38.777	-39:34:59.95	17.13	0.1833e
12	22:37:35.906	-39:34:59.91	18.39	0.2417
13	22:37:31.125	-39:36:07.02	17.23	0.0337e
14	22:37:33.581	-39:36:30.73	18.58	0.1305e
15	22:37:46.456	-39:35:07.23	18.71	0.2339e
16	22:37:58.464	-39:35:47.48	18.67	0.2489
17	22:37:47.504	-39:36:12.23	17.63	0.2499e
18	22:37:50.926	-39:35:59.23	18.78	0.2508e
19	22:37:47.870	-39:36:27.53	18.92	0.2498
20	22:38:20.761	-39:30:55.39	18.46	0.2064
21	22:38:21.946	-39:30:55.40	19.28	0.2408:
22	22:38:11.028	-39:30:54.51	19.73	0.1452e
23	22:37:43.169	-39:31:44.08	17.34	0.2428
24	22:37:53.760	-39:31:27.55	19.20	0.2400:
25	22:37:45.857	-39:32:05.32	16.91	0.2470
26	22:37:45.681	-39:31:33.72	18.63	0.2431
27	22:37:55.661	-39:31:40.68	18.93	0.2386e
28	22:37:57.083	-39:31:52.12	19.40	0.1521:
29	22:37:58.084	-39:33:04.46	17.62	0.0642e
30	22:38:05.073	-39:31:49.57	19.55	0.3006:
31	22:37:44.429	-39:31:58.03	19.63	0.2201:
32	22:37:43.081	-39:32:12.45	19.54	0.2476
33	22:37:47.015	-39:32:21.28	18.60	0.2454
34	22:37:50.214	-39:32:31.51	18.94	0.0937e
35	22:38:15.865	-39:32:51.71	19.46	0.2370:
36	22:38:08.583	-39:33:23.07	16.10	0.0935
37	22:38:01.804	-39:32:41.46	18.74	0.2015
38	22:37:43.675	-39:32:49.27	18.72	0.2472
39	22:37:53.666	-39:33:13.03	18.36	0.2479
40	22:38:12.434	-39:33:18.46	18.67	0.1537e
41	22:37:50.476	-39:33:25.65	19.01	0.5203
42	22:38:06.994	-39:34:06.52	18.37	0.2507
43	22:38:02.062	-39:34:25.33	17.61	0.2387
44	22:38:12.072	-39:34:15.58	19.11	0.2369e
45	22:38:05.687	-39:34:23.34	18.08	0.2387
46	22:38:03.541	-39:34:24.62	18.06	0.2383
47	22:37:50.431	-39:34:31.90	19.25	0.2491:
48	22:37:57.992	-39:34:54.18	17.25	0.1417
49	22:38:16.007	-39:34:59.36	17.71	0.2406
50	22:38:14.846	-39:34:53.31	19.33	0.2395:
51	22:37:52.823	-39:35:00.37	18.80	0.5200
52	22:38:16.927	-39:35:12.88	18.99	0.2399
53	22:38:17.395	-39:35:30.36	18.09	0.2414
54	22:38:21.365	-39:35:37.04	18.70	0.1719
55	22:38:11.867	-39:35:48.18	18.57	0.5360
56	22:37:34.415	-39:29:34.23	17.30	0.0714:
57	22:37:32.062	-39:29:55.14	18.78	0.0634e
58	22:37:57.019	-39:30:38.53	16.20	0.1593
59	22:38:02.148	-39:29:34.12	17.29	0.2509
60	22:38:05.393	-39:30:07.48	17.61	0.2493
61	22:37:42.809	-39:31:42.50	17.91	0.2395e

Table A.5. Redshifts obtained in the EISJ2241-3949 field.

	α (J2000)	δ (J2000)	I	z
1	22:41:23.435	-39:47:24.81	19.17	0.0633e
2	22:41:28.818	-39:47:36.55	19.63	0.0774e
3	22:41:20.065	-39:48:45.26	18.91	0.5941:
4	22:41:23.970	-39:49:13.76	17.88	0.1973
5	22:41:30.992	-39:49:16.69	19.06	0.3111
6	22:41:28.323	-39:49:33.32	18.84	0.3870
7	22:41:28.839	-39:50:02.85	19.80	0.1975e
8	22:41:29.825	-39:50:22.60	17.62	0.1254e
9	22:41:22.526	-39:52:11.82	18.55	0.1966e
10	22:41:29.861	-39:52:11.49	18.66	0.1984e
11	22:41:48.614	-39:52:00.83	17.92	0.1858
12	22:41:55.496	-39:51:54.89	17.27	0.1853
13	22:42:06.095	-39:47:31.71	17.44	0.1957
14	22:41:57.485	-39:47:36.01	18.92	0.2166
15	22:42:09.769	-39:48:03.26	17.72	0.2869
16	22:41:49.121	-39:47:52.42	18.82	0.1873
17	22:42:13.689	-39:48:10.61	19.79	0.3484e
18	22:42:02.616	-39:48:15.67	19.24	0.4681:
19	22:41:58.583	-39:48:28.68	18.74	0.1958:
20	22:41:52.025	-39:48:48.84	18.06	0.1857
21	22:42:16.432	-39:48:35.60	19.11	0.1956e
22	22:41:46.161	-39:48:33.22	18.02	0.1852
23	22:41:43.512	-39:48:30.01	19.75	0.1844e
24	22:42:08.747	-39:48:41.00	19.00	0.1411e
25	22:41:42.246	-39:49:07.87	17.27	0.1854
26	22:41:47.970	-39:48:41.88	19.40	0.2336e
27	22:41:36.231	-39:48:46.68	19.13	0.1842:
28	22:41:38.070	-39:48:49.68	18.00	0.1846e
29	22:41:40.585	-39:49:03.73	18.42	0.1835:
30	22:41:56.250	-39:48:46.91	19.90	0.1183e
31	22:42:03.609	-39:49:04.46	17.89	0.1966:
32	22:41:33.782	-39:49:11.73	18.70	0.5216:
33	22:41:39.520	-39:49:12.80	18.09	0.1860
34	22:41:34.573	-39:49:08.96	18.87	0.2464
35	22:41:34.078	-39:49:24.57	18.59	0.1953
36	22:42:10.067	-39:49:51.92	18.71	0.0667e
37	22:41:35.442	-39:50:07.36	18.62	0.1949
38	22:42:08.214	-39:50:31.87	19.67	0.3464e
39	22:42:04.918	-39:50:43.05	19.79	0.1876:
40	22:41:52.063	-39:51:13.20	19.21	0.1854e
41	22:42:05.836	-39:50:52.05	19.73	0.4682e
42	22:42:16.848	-39:51:29.66	19.21	0.2634:
43	22:42:02.333	-39:51:38.73	19.70	0.2982e
44	22:41:59.982	-39:51:38.76	18.99	0.1863e
45	22:42:16.533	-39:51:47.76	19.06	0.3093:
46	22:41:21.140	-39:47:16.34	18.68	0.1047e
47	22:41:56.216	-39:46:26.98	17.32	0.1485
48	22:41:40.202	-39:48:48.93	15.78	0.0631e
49	22:41:46.989	-39:48:56.02	16.89	0.1851e
50	22:41:39.926	-39:49:02.91	16.69	0.1855e
51	22:41:50.982	-39:49:08.76	18.34	0.1860
52	22:42:01.359	-39:51:21.86	17.99	0.1852

Table A.6. Redshifts obtained in the EISJ2243-4013 field.

	α (J2000)	δ (J2000)	I	z
1	22:42:58.579	-40:12:57.69	18.39	0.1488e
2	22:43:04.156	-40:12:53.82	19.86	0.3357:
3	22:42:59.935	-40:13:58.80	17.00	0.1973
4	22:42:49.475	-40:14:03.24	18.92	0.3568e
5	22:42:52.655	-40:14:18.01	16.97	0.1980
6	22:42:42.480	-40:14:33.05	18.48	0.1797:
7	22:42:39.148	-40:15:12.07	20.02	0.3358:
8	22:42:38.743	-40:15:15.53	18.47	0.3338
9	22:42:46.002	-40:15:25.53	19.00	0.2472e
10	22:42:46.732	-40:16:14.73	17.72	0.1817
11	22:43:16.006	-40:16:43.00	17.24	0.1844
12	22:43:12.558	-40:17:22.46	18.51	0.2709e
13	22:43:10.918	-40:12:20.53	18.13	0.1988e
14	22:43:26.840	-40:13:29.73	17.50	0.2112
15	22:43:07.330	-40:14:20.54	17.02	0.0289e
16	22:43:29.503	-40:15:05.60	18.19	0.2841
17	22:43:28.584	-40:15:22.96	19.04	0.2872:
18	22:43:32.696	-40:17:47.93	18.17	0.2992
19	22:43:05.941	-40:15:32.09	17.30	0.1858:

Table A.7. Redshifts obtained in the EISJ2243-4025 field.

	α (J2000)	δ (J2000)	I	z
1	22:43:02.589	-40:25:32.92	17.56	0.1280
2	22:43:22.969	-40:25:44.63	16.46	0.2454
3	22:43:15.546	-40:24:53.99	17.54	0.1860
4	22:43:21.024	-40:24:54.71	19.41	0.5571:
5	22:43:11.394	-40:25:03.30	19.28	0.2230e
6	22:43:22.063	-40:25:20.52	18.69	0.5557
7	22:43:27.892	-40:25:22.16	19.02	0.5555:
8	22:43:14.397	-40:25:33.94	19.48	0.2472
9	22:43:20.170	-40:25:47.12	18.28	0.1705
10	22:43:09.981	-40:25:42.46	18.91	0.2846
11	22:43:23.168	-40:25:50.28	19.20	0.2457
12	22:43:20.295	-40:26:19.94	18.37	0.1708:
13	22:43:16.445	-40:26:40.08	17.82	0.2462
14	22:43:10.496	-40:26:26.10	18.03	0.2883
15	22:43:18.653	-40:26:19.68	19.30	0.2450
16	22:43:22.568	-40:26:24.03	19.09	0.2483:
17	22:43:14.004	-40:26:34.69	18.89	0.1862
18	22:43:25.150	-40:26:49.23	19.48	0.3349
19	22:43:12.469	-40:27:39.89	18.97	0.1887
20	22:43:33.983	-40:23:13.05	18.03	0.2470
21	22:43:47.940	-40:24:02.55	16.64	0.1702
22	22:43:25.769	-40:23:59.61	17.16	0.0287e
23	22:43:28.254	-40:24:11.48	18.94	0.2464
24	22:43:47.314	-40:24:35.09	19.65	0.1708:
25	22:43:40.336	-40:24:55.50	18.81	0.2456
26	22:43:50.863	-40:25:18.52	18.92	0.3939:
27	22:43:31.794	-40:25:31.31	19.08	0.2468:
28	22:43:50.478	-40:25:47.09	19.32	0.2457:
29	22:43:34.421	-40:26:02.31	17.65	0.2470
30	22:43:29.802	-40:26:06.90	17.72	0.2445
31	22:43:48.674	-40:26:10.08	18.65	0.2004e
32	22:43:36.312	-40:26:31.21	17.71	0.2300
33	22:43:45.191	-40:26:37.52	17.62	0.2456
34	22:43:38.596	-40:26:45.27	19.97	0.2483
35	22:43:36.738	-40:26:48.84	18.90	0.2290
36	22:43:34.854	-40:26:53.28	19.26	0.2433
37	22:43:41.967	-40:27:21.12	19.30	0.5083:
38	22:43:59.485	-40:25:07.72	19.60	0.2283e
39	22:44:00.475	-40:26:47.86	19.24	0.2448:
40	22:43:55.060	-40:26:53.34	19.41	0.2465:
41	22:43:53.702	-40:28:16.08	18.93	0.1704e

Table A.8. Redshifts obtained in the EISJ2244-3955 field.

	α (J2000)	δ (J2000)	I	z
1	22:44:25.351	-39:55:46.15	18.49	0.0971e
2	22:44:30.258	-39:55:44.12	17.36	0.1946
3	22:44:32.002	-39:56:29.17	17.75	0.1268e
4	22:44:07.574	-39:56:44.92	19.14	0.5408e
5	22:44:07.473	-39:56:55.79	18.15	0.1267e
6	22:44:02.723	-39:57:40.29	19.70	0.1467e
7	22:44:01.253	-39:58:28.25	18.58	0.2572
8	22:44:31.219	-39:58:26.43	19.44	0.0952e
9	22:44:58.067	-39:55:50.29	17.76	0.0888:
10	22:44:57.551	-39:55:49.89	19.62	0.2440e
11	22:44:47.948	-39:56:27.23	18.22	0.1894e
12	22:44:55.449	-39:56:40.62	19.91	0.3072:
13	22:44:09.950	-39:54:21.14	18.03	0.1911e
14	22:44:04.950	-39:55:42.84	16.60	0.0644e
15	22:44:10.926	-39:55:27.38	18.31	0.2840
16	22:44:06.342	-39:55:35.07	19.45	0.0640e
17	22:44:21.356	-39:54:46.90	16.00	0.0778
18	22:44:28.170	-39:54:08.12	19.83	0.0991e
19	22:44:36.558	-39:54:20.80	19.91	0.3405e
20	22:44:23.840	-39:54:59.75	19.91	0.3846e
21	22:44:26.526	-39:55:46.61	16.88	0.0980e
22	22:44:40.740	-39:54:01.54	18.55	0.1253e
23	22:44:52.997	-39:54:31.20	17.79	0.2000

Table A.9. Redshifts obtained in the EISJ2245-3952 field.

	α (J2000)	δ (J2000)	I	z
1	22:44:59.583	-39:52:51.79	16.82	0.0510e
2	22:44:52.968	-39:53:07.17	19.34	0.2452
3	22:44:56.437	-39:53:19.90	19.58	0.0516e
4	22:45:01.519	-39:53:32.13	18.91	0.0516e
5	22:44:59.830	-39:53:49.23	19.88	0.1247e
6	22:44:52.997	-39:54:31.20	17.79	0.1992e
7	22:45:02.722	-39:50:52.31	19.54	0.4448
8	22:45:24.094	-39:51:53.41	16.37	0.1006e
9	22:45:05.662	-39:51:21.45	19.28	0.1458e
10	22:45:19.808	-39:51:54.02	19.55	0.4488:
11	22:45:22.737	-39:51:43.46	18.91	0.4332
12	22:45:06.172	-39:51:57.88	18.63	0.1378
13	22:45:12.663	-39:52:55.21	15.93	0.1379
14	22:45:20.118	-39:52:05.60	19.19	0.1955e
15	22:45:02.998	-39:52:29.19	18.59	0.1989
16	22:45:17.400	-39:52:32.24	19.26	0.1589e
17	22:45:07.731	-39:53:36.03	16.96	0.1381
18	22:45:14.664	-39:54:39.09	19.50	0.0739e
19	22:45:15.889	-39:55:15.73	19.79	0.4022:
20	22:45:32.116	-39:52:04.63	19.21	0.0926e
21	22:45:41.256	-39:53:47.87	18.54	0.2645
22	22:45:30.622	-39:54:06.04	17.15	0.1250e
23	22:45:39.761	-39:54:07.76	18.22	0.2645
24	22:45:40.753	-39:54:22.15	19.39	0.3359
25	22:45:41.977	-39:54:23.27	20.00	0.3367e
26	22:45:28.141	-39:55:13.12	19.15	0.1009e
27	22:45:45.666	-39:54:58.83	19.22	0.2444
28	22:45:27.931	-39:50:10.78	18.75	0.3842
29	22:45:35.004	-39:51:37.30	17.57	0.1550e
30	22:45:30.001	-39:50:47.31	19.88	0.1115e

Table A.10. Redshifts obtained in the EISJ2246-4012A field.

	α (J2000)	δ (J2000)	I	z
1	22:46:07.293	-40:16:20.60	19.00	0.3328e
2	22:46:50.798	-40:11:57.58	19.24	0.1543e
3	22:46:33.560	-40:12:29.75	19.96	0.2066e
4	22:46:39.449	-40:12:56.08	16.96	0.0677e
5	22:46:49.692	-40:13:36.72	18.07	0.0665e
6	22:46:23.548	-40:13:04.92	17.14	0.2306
7	22:47:00.767	-40:13:16.35	17.35	0.1765
8	22:46:37.765	-40:13:12.67	19.98	0.2124e
9	22:46:57.625	-40:13:20.56	19.80	0.1259e
10	22:46:19.746	-40:13:51.63	18.43	0.1509e
11	22:46:38.885	-40:14:03.42	17.54	0.2115:
12	22:46:35.818	-40:14:06.29	18.17	0.1254e
13	22:46:21.656	-40:14:42.76	17.84	0.2437
14	22:46:33.510	-40:14:37.85	18.86	0.2470
15	22:46:28.914	-40:14:35.56	18.98	0.3105
16	22:46:22.334	-40:14:39.38	19.45	0.4376:
17	22:46:20.730	-40:14:51.75	19.00	0.2451
18	22:46:45.431	-40:15:58.05	15.95	0.1480
19	22:46:37.105	-40:15:25.85	19.86	0.1533e
20	22:46:31.115	-40:15:22.71	19.21	0.2443
21	22:46:45.531	-40:15:28.07	18.56	0.1463e
22	22:46:18.711	-40:15:31.00	19.87	0.2419e
23	22:46:14.966	-40:15:42.79	19.55	0.2155e
24	22:46:25.009	-40:15:45.13	19.13	0.3368
25	22:46:54.021	-40:16:19.92	16.96	0.1766
26	22:46:26.547	-40:15:58.21	18.81	0.2448
27	22:46:35.009	-40:16:00.80	19.01	0.3103:
28	22:46:47.069	-40:16:05.67	18.12	0.1470e
29	22:46:42.441	-40:16:22.79	19.39	0.2923e
30	22:47:03.898	-40:12:47.35	19.84	0.1099
31	22:47:03.269	-40:14:00.30	19.19	0.1756:
32	22:46:31.533	-40:14:13.92	17.20	0.3122e
33	22:47:01.051	-40:13:07.60	18.89	0.1357